*Progress In Electromagnetics Research, PIER 67, 297–316, 2007*

# CHARACTERISTICS OF AN OFFSET LONGITUDINAL/TRANSVERSE SLOT COUPLED CROSSED WAVEGUIDE JUNCTION USING MULTIPLE CAVITY MODELING TECHNIQUE CONSIDERING THE $TE_{00}$ MODE AT THE SLOT APERTURE

**S. Das, A. Chakrabarty, and A. Chakraborty**

Department of Electronics and Electrical Communication Engineering
Indian Institute of Technology - Kharagpur
West Midnapore, West Bengal, PIN-721302, India

**Abstract**—A moment method analysis of a broad wall slot coupled crossed rectangular waveguide junction has been presented in this paper. The coupling slot is longitudinal/transverse and offset from the centre lines of the guides. The integral equations, governing the characteristics of the device, have been obtained using Multiple Cavity Modeling Technique, taking into account of the finite wall thickness and the $TE_{00}$ mode at the slot apertures and have been solved using Moment Method to obtain the aperture distribution. The normalized resonant lengths/complex S-parameters have been calculated from this field distribution for different guide height/slot offsets/slot widths/slot thickness of the longitudinal/transverse slot over the frequency band. Numerical data, thus obtained, have been compared with measured/literature available/CST Microwave Studio Simulated data. The theory has been validated by the reasonable agreement obtained between them. It has been shown that, neglecting the $TE_{00}$ mode at the slot apertures can adversely effect the estimation of the resonant frequency and equivalent network parameters.

## 1. INTRODUCTION

Longitudinal/transverse couplers are widely used for transferring power from a main waveguide to another crossed waveguide or branch waveguide. The longitudinal slot behaves nearly as a shunt element whereas the transverse slot behaves as a series element and that is why a longitudinal/transverse slot coupled crossed waveguide junctions is also called a shunt - series coupler. The offset of the slots controls the

power coupled to the crossed waveguide whereas the length of the slot determines the resonant frequency.

The slot coupler was initially studied by Watson [1]. He derived the approximate solutions for several equivalent circuit of the cross coupler. Later Vu Khac [2] used method of moment to obtain more precise result for the longitudinal/transverse slot coupler. The effect of wall thickness was ignored in his analysis. Harrington and Mautz [3] also presented a general network formulation for the aperture problems using method of moments. Rengarajan [4] also used method of moments to analyze the longitudinal/transverse slot coupled crossed waveguide junction considering the finite wall thickness and obtained the pertinent integral equations to obtain the aperture electric field. He considered that the transverse slot is centered and did not analyze the effect of transverse slot offsets and also neglected the existence of $TE_{00}$ mode at the slot aperture. Park et al. [5] investigated the thick shunt-series coupling slots by solving pertinent integral equation for the aperture field using pulse basis function and point matching technique. Results on the resonant length and resonant conductance in the waveguide, containing the shunt slot, were presented. Studies on higher order mode coupling between a thick longitudinal/transverse coupling slot and a pair of straddling radiating slots in the crossed waveguide were done by Senior [6] using an integral equation formulation. He used piecewise sinusoidal Galerkin and Global Galerkin method to solve the integral equations. Wu [7] analyzed broad wall longitudinal/transverse slot coupler using Finite Difference Time Domain Technique considering the slot wall thickness.

In this paper Multiple Cavity Modeling Technique (MCMT) [8] has been applied to study the longitudinal/transverse slot coupled waveguide cross coupler considering the wall thickness and $TE_{00}$ mode at the slot apertures. The existence of this mode in longitudinal slot radiators was first reported by Vu Khac and Carson [9]. Gupta, Chakraborty and Das [10] also reported on the effects of inclusion of the contribution due to this mode on the characteristics of broad wall longitudinal slot radiators. The $TE_{00}$ mode has a more significant effect on the characteristics of the waveguide couplers, which has been reported by Styanarayana and Chakraborty [11, 12]. Though not mentioned explicitly, the contribution of this mode was considered by some researchers, as given in the literature [13, 14]. Some more discussion on this mode is given in the literature [15].

The normal rectangular waveguide modes are formulated for zero electric fields on the waveguide walls. The corresponding magnetic field is maximum on the waveguide walls and zero at the center of the waveguide. When a slot is milled on the waveguide wall it creates a

disturbance in the field structure. The electric field on the waveguide walls in this region is no longer zero and has a finite value. The field in this non-conventional lossy rectangular waveguide region when expressed as a set of orthogonal functions of those regular rectangular waveguide modes, this particular $TE_{00}$ mode (which is also a solution of the Helmholtz Equation satisfying the boundary conditions near the slot region) arises. This component when integrated over the cross-section of the rectangular waveguide results in a non-zero value, which supports the existence of the aperture field. This component of longitudinal magnetic field may be assumed to have a path closed through the longitudinal components of the slot region and that of the tangential component of the other side of the slot. It should be noted in this connection, that in the case of an aperture in the transverse plane the aperture field is supported by the regular rectangular waveguide magnetic fields itself and the existence of this mode does not arise. The characteristics of this $TE_{00}$ mode are as follows: 1. This mode has an axial magnetic field only, which is constant all over the corresponding waveguide cross section. 2. The corresponding cut-off wave number vanishes. 3. The mode exists only for the longitudinal magnetic current on the waveguide wall.

## 2. PROBLEM FORMULATION

Figure 1 shows the three dimensional view of the shunt/series coupled waveguide cross coupler. The main waveguide is designated by port

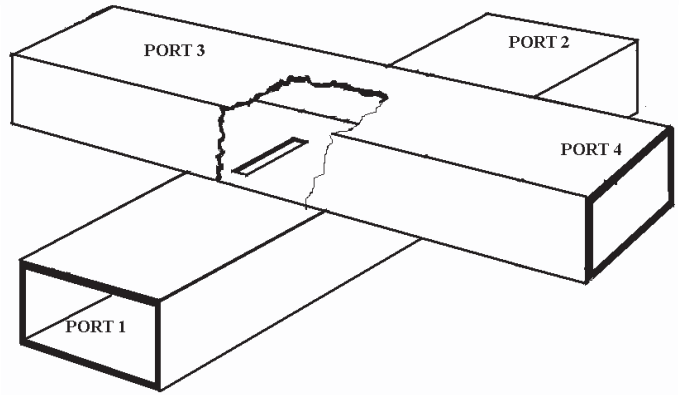


**Figure 1.** Three dimensional views of a shunt / series coupled crossed waveguide junction.

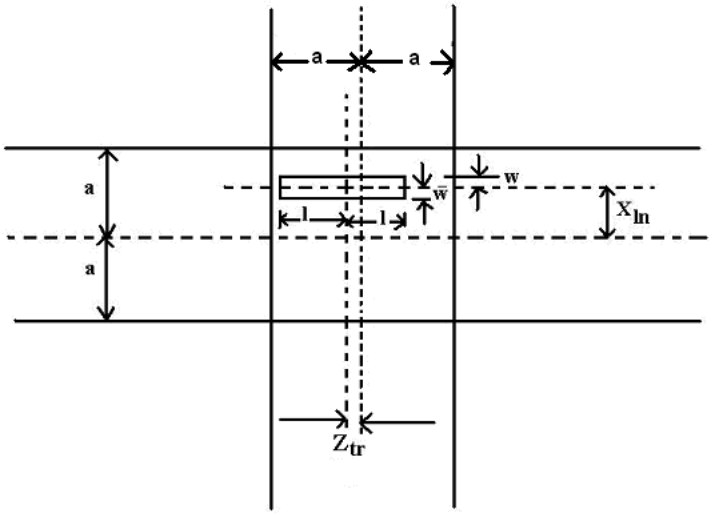


**Figure 2.** Position details of the slot and its dimensions of a shunt/series coupled crossed waveguide junction.

1 and port 2 whereas the crossed branch waveguide is designated by port 3 and port 4. A coupling slot is milled in the common broad wall of the two waveguide. Figure 2 shows the location of the slot which is offset by an amount $X_{ln}$ from the center line of the main waveguide and by an amount $Z_{tr}$ from the center line of the branch waveguide and the slot is of length $2l$ and width $2w$. $2t$ is the common wall thickness or the slot thickness. Both the waveguides are assumed to be composed of perfectly conducting walls and to be filled with homogeneous isotropic lossless dielectric. From Figure 3 it may be noted that the structures have three regions, namely, two waveguide regions and one cavity region. The interfacing apertures between different regions have been replaced by equivalent magnetic current densities. The magnetic current distribution in aperture 1 is $M_z^{aperture1}$ whereas $M_z^{aperture2}$ is the magnetic current distribution in aperture 2. Applying the continuity of the tangential component of the magnetic field across the aperture 1 and aperture 2 we get the boundary conditions respectively as:

$$H_z^{wvg\_m}\left(M_z^{aperture1}\right)+H_z^{cty}\left(M_z^{aperture1}\right)-H_z^{cty}\left(M_z^{aperture2}\right)=H_z^{inc\_m} \tag{1}$$

$$-H_z^{cty}\left(M_z^{aperture1}\right)+H_z^{cty}\left(M_z^{aperture2}\right)+H_z^{wvg\_b}\left(M_z^{aperture2}\right)=0 \tag{2}$$

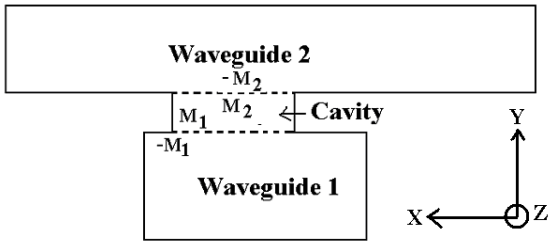


**Figure 3.** Details of region and magnetic currents in a shunt/series coupled crossed waveguide junction.

when the excitation is given through main waveguide and

$$H_z^{wvg\_m}\left(M_z^{aperture1}\right)+H_z^{cty}\left(M_z^{aperture1}\right)-H_z^{cty}\left(M_z^{aperture2}\right)=0 \quad (3)$$

$$-H_z^{cty}\left(M_z^{aperture1}\right)+H_z^{cty}\left(M_z^{aperture2}\right)+H_z^{wvg\_b}\left(M_z^{aperture2}\right)=H_z^{inc\_b} \quad (4)$$

when the excitation is through branch waveguide. In equations (1)–(4), the magnetic currents at the apertures are assumed to be

$$M_z^{aperture}=\sum_{p=1}^{\infty}A_{pz}^{aperture}m_{pz}^{aperture} \quad (5)$$

where $A_{pz}^{aperture}$ are basis coefficients and the basis function $m_{pz}^{aperture}$ $(p=1,2,3\ldots M)$ are defined by

$$m_{pz}^{aperture1}=\begin{cases}\sin\left\{\dfrac{p\pi}{2l}(z+l)\right\}\delta(y-b) & \begin{array}{c}-l\le z\le l\\ X_{ln}-w\le x\le X_{ln}+w\\ \text{(for main waveguide)/}\\ -w\le x\le w\text{ (for cavity)}\end{array}\\ 0 & \text{elsewhere}\end{cases} \quad (6)$$

and

$$m_{pz}^{aperture2}=\begin{cases}\sin\left\{\dfrac{p\pi}{2l}(z-Z_{tr}+l)\right\}\delta(y+b) & \begin{array}{c}Z_{tr}-l\le z\le Z_{tr}+l\\ \text{(for branch waveguide)/}\\ -l\le z\le l\text{ (for cavity)}\\ -w\le x\le w\end{array}\\ 0 & \text{elsewhere}\end{cases} \quad (7)$$

Where $2a \times 2b$ is the cross sectional dimension of the waveguide.

The $Z$-component of incident magnetic field at the main waveguide is the dominant $TE_{10}$ mode and is given by

$$H_z^{inc\_m} = -j \sin\left(\frac{\pi x}{2a}\right) e^{-j\beta z} \tag{8}$$

for the branch waveguide the same is given by

$$H_x^{inc\_b} = \frac{\pi}{2ja\beta} \sin\left(\frac{\pi z}{2a}\right) e^{-j\beta x} \tag{9}$$

$$H_z^{inc\_b} = -\cos\left(\frac{\pi z}{2a}\right) e^{-j\beta x} \tag{10}$$

The tangential component of the magnetic field scattered inside the cavity is given by [8]

$$H_z^{cty}(M_z) = \begin{cases} \dfrac{j\omega\varepsilon}{k^2} \displaystyle\sum_m \sin\left\{\frac{m\pi}{2l}(z+l)\right\} \cot\{2\Gamma_{m0}t\} & \text{if } m = p \\ & \text{and } n = 0 \\ 0 & \text{elsewhere} \end{cases} \tag{11}$$

The magnetic field scattered inside the cavity region due to the source is determined by using cavity Green's function of the electric vector potential. The cavity Green's function has been derived by solving the Helmholtz equation for the electric vector potential for the unit magnetic current source.

The scattered magnetic fields in the waveguide region due to the presence of the magnetic current densities at the slot apertures has been calculated using waveguide Green's function [16] and is given by

$$\begin{aligned} H_z^{wvg\_m}(M_z) = \sum_{m=0}^{\infty} \sum_{n=0}^{\infty} & \frac{j\varepsilon_m \varepsilon_n w}{2k\eta\gamma_{mn}^2 ab} \frac{\cos(n\pi)}{1+S^2(p)} \cos\left\{\frac{m\pi}{2a}(x_{ln}+a)\right\} \\ & \sin c\left\{\frac{m\pi}{2a}w\right\} \left[\left\{k^2 - \left(\frac{p\pi}{2l}\right)^2\right\} \sin\left\{\frac{p\pi}{2l}(z+l)\right\}\right. \\ & \left. + \left(k^2+\gamma_{mn}^2\right) S(p) e^{-\gamma_{mn} l} \left\{\begin{matrix} -\sinh(\gamma_{mn} z) & p \text{ even} \\ \cosh(\gamma_{mn} z) & p \text{ odd} \end{matrix}\right\}\right] \\ & \cos\left\{\frac{m\pi}{2a}(x+a)\right\} \cos\left\{\frac{n\pi}{2b}(y+b)\right\} \end{aligned} \tag{12}$$

for the main waveguide and

$$H_z^{wvg\_b}(M_z) \frac{l}{2jabk\eta} \sum_{m=0}^{\infty} \sum_{n=0}^{\infty} \frac{\varepsilon_n \cos(n\pi)}{\gamma_{mn}^2} F(p,m) \sin\left\{\frac{m\pi}{2a}(z+a)\right\}$$

$$\cos\left\{\frac{n\pi}{2b}(y+b)\right\}\left\{k^2-\left(\frac{m\pi}{2a}\right)^2\right\}\left[1-e^{-\gamma_{mn}w}\cosh(\gamma_{mn}x)\right] \quad (13)$$

for the branch waveguide.

Where

$$S(p)=\frac{p\pi}{2l\gamma_{mn}} \quad (14)$$

and

$$F(p,m)=\cos\left[\frac{\pi}{2}\left\{\left(\frac{p}{l}-\frac{m}{a}\right)Z_{tr}+\frac{p}{l}(l-Z_{tr})-m\right\}\right]\sin c\left\{\frac{\pi l}{2}\left(\frac{p}{l}-\frac{m}{a}\right)\right\}$$
$$-\cos\left[\frac{\pi}{2}\left\{\left(\frac{p}{l}+\frac{m}{a}\right)Z_{tr}+\frac{p}{l}(l-Z_{tr})+m\right\}\right]\sin c\left\{\frac{\pi l}{2}\left(\frac{p}{l}+\frac{m}{a}\right)\right\} \quad (15)$$

Applying Galerkin's method to the boundary conditions where the same entire domain sinusoidal function is used for testing the expanded magnetic fields, the final form will be a matrix equation of the form For main waveguide excitation:

$$[L_{11}]\{A^{aperture1}\}+[L_{12}]\{A^{aperture2}\}=\{L_{inc\_m}\} \quad (16)$$
$$[L_{21}]\{A^{aperture1}\}+[L_{22}]\{A^{aperture2}\}=\{0\} \quad (17)$$

For branch waveguide excitation:

$$[L_{11}]\{A^{aperture1}\}+[L_{12}]\{A^{aperture2}\}=\{0\} \quad (18)$$
$$[L_{21}]\{A^{aperture1}\}+[L_{22}]\{A^{aperture2}\}=\{L_{inc\_b}\} \quad (19)$$

Where

$$L_{11/22}(p,q) = \iint\limits_{aperture\,1} w_q^{aperture1}\cdot\left\{H_z^{wvg\_m/b}\left(m_{pz}^{aperture1}\right) + H_z^{cty}\left(m_{pz}^{aperture1}\right)\right\}dxdz \quad (20)$$

$$L_{ij}(p,q) = \iint\limits_{aperture\,i} w_q^{aperturei}\cdot H_z^{cty}\left(m_{pz}^{aperturej}\right)dxdz \quad (21)$$

$$L_{inc\_m/b}(i,q) = \iint\limits_{aperture\,1} w_q^{aperturei}\cdot H_z^{inc\_m/b}dxdz \quad (22)$$

Solving the matrix equation the basis coefficients can be calculated. The $+Z$ and $-Z$ directed scattered field inside the main waveguide at

the $z = 0$ plane is given by

$$H^{-}_{z,main}(x,y,0) = -j\frac{\pi^2 w}{4a^3bk\eta\beta^2}\sum_{p=1}^{M} A_p^{aperture1}\sin\left(\frac{\pi x_{ln}}{2a}\right)\sin c\left(\frac{\pi w}{2a}\right) \frac{S(p)}{1+S^2(p)}\left\{\begin{array}{ll}\cos(\beta l) & p \text{ odd}\\ j\sin(\beta l) & p \text{ even}\end{array}\right\}\sin\left(\frac{\pi x}{2a}\right) \quad (23)$$

and

$$H^{+}_{z,main}(x,y,0) = -j\frac{\pi^2 w}{4a^3bk\eta\beta^2}\sum_{p=1}^{M} A_p^{aperture1}\sin\left(\frac{\pi x_{ln}}{2a}\right)\sin c\left(\frac{\pi w}{2a}\right) \frac{S(p)}{1+S^2(p)}\left\{\begin{array}{ll}\cos(\beta l) & p \text{ odd}\\ -j\sin(\beta l) & p \text{ even}\end{array}\right\}\sin\left(\frac{\pi x}{2a}\right) \quad (24)$$

respectively. Similarly the $+X$ and $-X$ component of the dominant mode scattered field inside the branch waveguide at $x = 0$ plane is given by

$$H^{-/+}_{x,branch}(0,y,z) = \frac{\pi l\sin(\beta w)}{4a^3bk\eta\beta}\sum_{p=1}^{M} A_p^{aperture2}F(p,1)\sin\left(\frac{\pi x}{2a}\right) \quad (25)$$

The dominant mode reflection coefficients in the main waveguide can be calculated as

$$\begin{aligned}\Gamma_{main} &= \frac{H_z^{-}}{H_z^{inc\_m}}\\ &= \frac{\pi^2 w}{4a^3bk\eta\beta^2}\sin\left(\frac{\pi x_{ln}}{2a}\right)\sin c\left(\frac{\pi w}{2a}\right)\\ &\quad \sum_{p=1}^{M} A_p^{aperture1}\frac{S(p)}{1+S^2(p)}\left\{\begin{array}{ll}\cos(\beta l) & p \text{ odd}\\ j\sin(\beta l) & p \text{ even}\end{array}\right\}\end{aligned} \quad (26)$$

The transmission coefficient at port 2 due to excitation at port 1 is given by

$$\begin{aligned}T_{21} &= \left.\frac{H_z^{inc\_m} + H^{+}_{z,main}}{H_z^{inc\_m}}\right|_{z=0}\\ &= 1 + \frac{\pi^2 w}{4a^3bk\eta\beta^2}\sin\left(\frac{\pi x_{ln}}{2a}\right)\sin c\left(\frac{\pi w}{2a}\right)\\ &\quad \sum_{p=1}^{M} A_p^{aperture2}\frac{S(p)}{1+S^2(p)}\left\{\begin{array}{ll}\cos(\beta l) & p \text{ odd}\\ -j\sin(\beta l) & p \text{ even}\end{array}\right\}\end{aligned} \quad (27)$$

and the transmission coefficient at port 3 and port 4 is given by

$$T_{31} = -\frac{\pi l \sin(\beta w)}{4a^2 bk\eta\beta} \sum_{p=1}^{M} A_p^{aperture2} F(p,1) \tag{28}$$

$$T_{41} = \frac{\pi l \sin(\beta w)}{4a^2 bk\eta\beta} \sum_{p=1}^{M} A_p^{aperture2} F(p,1) \tag{29}$$

Similarly the S-parameters of the circuit when excited by a dominant mode in the branch waveguide is given by

$$\Gamma_{branch} = \left.\frac{H_{x,branch}^{-}}{H_x^{inc\_b}}\right|_{z=0} = -\frac{l \sin(\beta w)}{2abk\eta} \sum_{p=1}^{M} A_p^{aperture2} F(p,1) \tag{30}$$

$$T_{34} = \left.\frac{H_x^{+} + H_x^{inc\_b}}{H_x^{inc\_b}}\right|_{z=0} = 1 - \frac{l \sin(\beta w)}{2abk\eta} \sum_{p=1}^{M} A_p^{aperture2} F(p,1) \tag{31}$$

$$T_{14} = \frac{\pi^2 w}{4a^2 bk\eta\beta^2} \sin\left(\frac{\pi x_{ln}}{2a}\right) \sin c\left(\frac{\pi w}{2a}\right) \sum_{p=1}^{M} A_p^{aperture2} \frac{S(p)}{1+S^2(p)} \left\{ \begin{array}{ll} \cos(\beta l) & p \text{ odd} \\ -j\sin(\beta l) & p \text{ even} \end{array} \right\} \tag{32}$$

The equivalent shunt admittance and series impedance, as shown in Figure 4, can be calculated from the complex reflection coefficient using the following equations [16]

$$Y = -\frac{2\Gamma}{1+\Gamma} \tag{33}$$

$$Z = \frac{2\Gamma}{1-\Gamma} \tag{34}$$

Stern and Elliot [17] explained the importance of the resonant length of a slot. For compound radiating and coupling slots, resonance has been defined by the phase relation of the forward scattered $TE_{10}$ mode with the incident $TE_{10}$ mode [18, 19]. This condition corresponds to a maximum of energy radiated or coupled into the branch waveguide, and this condition is applicable for the shunt and series elements also [1, 4, 7]. This definition of resonance for the longitudinal/transverse coupling slot is consistent with compound coupling slot and is also consistent with compound coupling slot results for the limiting case of zero tilt [19]. The second definition of resonance is based on the

condition that the backward scattered $TE_{10}$ mode is out of phase with the incident $TE_{10}$ mode. This definition has been employed for shunt-type elements, longitudinal/transverse slot couplers, and longitudinal radiating slots [5, 6, 17]. Rengarajan [4] mentioned that the resonant length based on the forward scattered wave phase is difficult to determine experimentally whereas that based on the backscattered wave phase is easy to measure.

The definitions given above are same for an ideal shunt/series element [4]. Since longitudinal radiating slots and coupling slots do not behave as perfect shunt elements [20], the two definitions results in different slot lengths - the resonance definition based on the forward scattered wave phase predicts slightly longer slots. The shunt representation also becomes poorer for smaller waveguide dimensions and larger offsets. So the resonance conditions are not perfectly true to define the resonant length of such circuits.

Since the slots are radiating or coupling power to a branch waveguide, they can be represented by a lossy transmission line with distributive circuit parameters. So the more exact equivalent circuit of a slot coupled crossed waveguide junction is a Tee/Pi network rather than a simple single shunt/series element and is shown in Figure 4.

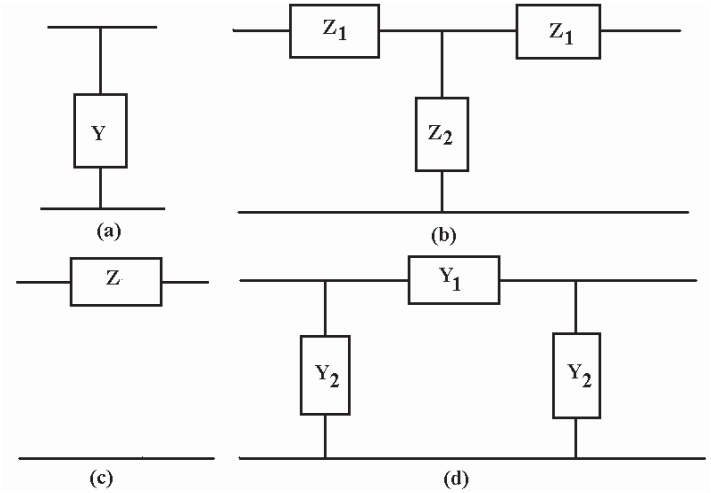


**Figure 4.** (a) Equivalent shunt model (b) Equivalent tee model (c) Equivalent series model and (d) Equivalent Pi model of slot coupled crossed waveguide junction.

The equivalent circuit parameters are goven by

$$Y_1 = \frac{1-\Gamma-T}{1+\Gamma+T} \tag{35a}$$

$$Y_2 = \frac{2T}{(1+\Gamma+T)(1+\Gamma-T)} \tag{35b}$$

$$Z_1 = \frac{1+\Gamma-T}{1-\Gamma+T} \tag{35c}$$

$$Z_2 = \frac{2T}{(1-\Gamma+T)(1-\Gamma-T)} \tag{35d}$$

For accurate determination of the resonant length, the resonance conditions must be defined in terms of the above Tee/Pi network equivalent circuits.

## 3. NUMERICAL RESULTS

### 3.1. Resonant Characteristics of the Slot

Figure 5 shows the comparison of normalized resonant length data for the longitudinal/transverse slot coupler with $2a = 22.86\,\text{mm}$, $2w = 1.5875\,\text{mm}$, $Z_{tr} = 0\,\text{mm}$ and $f = 9.3\,\text{GHz}$ as a function of slot offset $X_{ln}$ as obtained using this theory and Wu [7]. The effects of waveguide

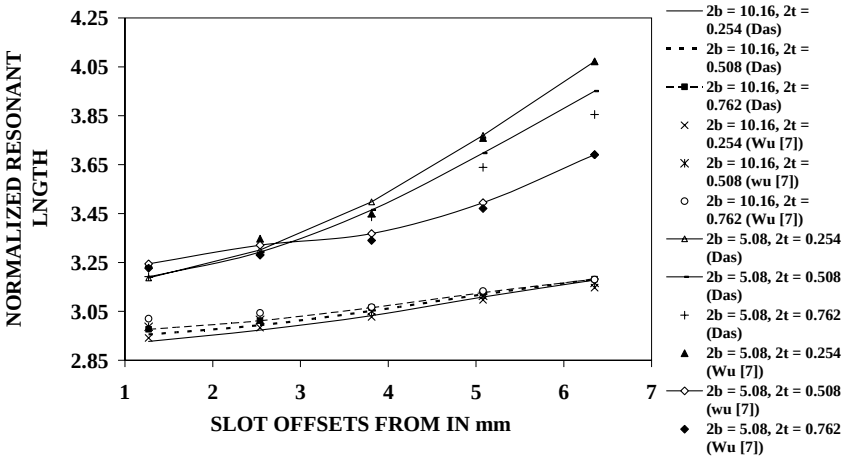


**Figure 5.** Plot of normalized resonant length as a function of slot offsets in main waveguide for different waveguide height and slot thickness.

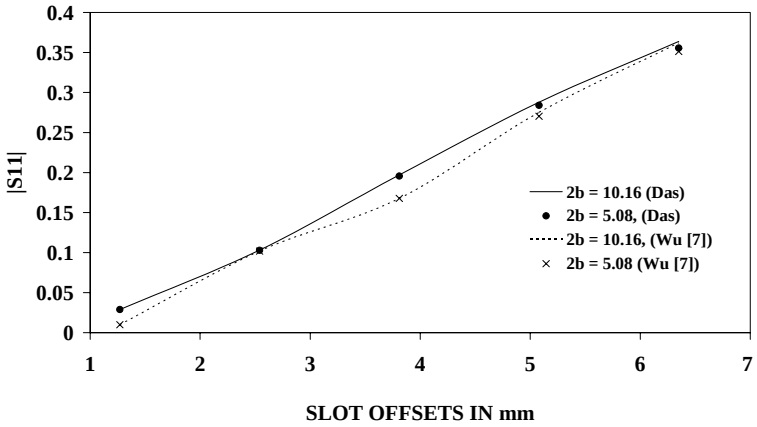


**Figure 6.** Plots of magnitude of reflection coefficient at resonance as a function of slot offsets in main waveguide for different guide height.

size $2b$ and wall thickness $2t$ are also studied in the figure. Figure 6 shows the plot of absolute value of reflection coefficient at resonance for a longitudinal/transverse slot coupled waveguide junction with $2a = 22.86\,\text{mm}$, $2w = 1.5875\,\text{mm}$, $2t = 0.762\,\text{mm}$, $Z_{tr} = 0\,\text{mm}$ and $f = 9.3\,\text{GHz}$ as a function of slot offset $X_{ln}$ considering $\text{TE}_{00}$ mode. The data obtained by Wu [7] has been plotted in the same figure for comparison. The plot of normalized resonant length is plotted in Figure 7 as a function of frequency for $2a = 22.86\,\text{mm}$, $2w = 1.5876\,\text{mm}$, $2t = 0.762\,\text{mm}$ and $Z_{tr} = 0\,\text{mm}$. The effects of waveguide size 2b and slot offsets $X_{ln}$ are also studied in the figure. The plot of normalized resonant length is plotted in Figure 8 as a function of slot offset for $2a = 22.86\,\text{mm}$, $2t = 0.762\,\text{mm}$, $Z_{tr} = 0\,\text{mm}$ and $f = 9.3\,\text{GHz}$. The effects of waveguide size $2b$ and slot width $2w$ are also studied in the figure.

### 3.2. Off Resonant Characteristics of the Slot

Scattering parameters for longitudinal/slot coupled waveguide junction with: $2a = 22.86\,\text{mm}$, $2b = 10.16\,\text{mm}$, $2t = 0.762\,\text{mm}$, $2w = 1.5875\,\text{mm}$, $X_{ln} = 3.81\,\text{mm}$ and $Z_{tr} = 0\,\text{mm}$ has been calculated and has been compared with that obtained by Wu [7] in Figure 9. Resonance frequency was adjusted to 9.3 GHz by changing the slot length.

The effect of $\text{TE}_{00}$ mode on the equivalent shunt/series parameters is shown in Figure 10 to 11. The slot dimensions for this case is chosen

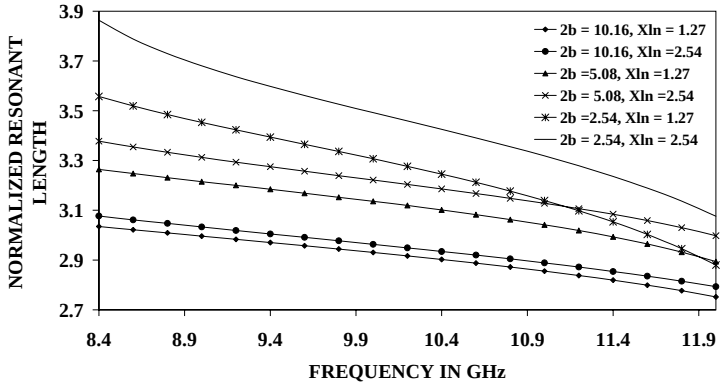


**Figure 7.** Plot of normalized resonant length as a function of frequency for different guide height and offsets in main waveguide.

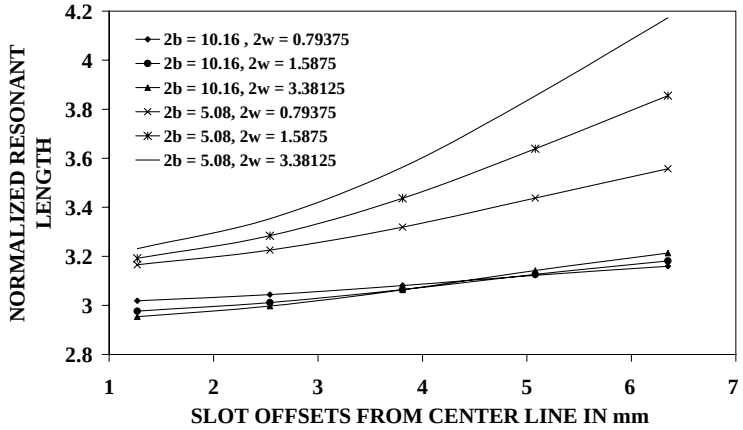


**Figure 8.** Plot of normalized resonant length as a function of slot offsets in main waveguide for different guide height and slot widths.

to be $2a = 22.86\,\text{mm}$, $2b = 10.16\,\text{mm}$, $2l = 16\,\text{mm}$, $2w = 0.8\,\text{mm}$, $X_{ln} = 8\,\text{mm}$ and $Z_{tr} = 2\,\text{mm}$. The comparison of shunt and tee model/series and pi is shown in Figures 12 and 13 for a slot with $2a = 22.86\,\text{mm}$, $2b = 10.16\,\text{mm}$, $2t = 1.27\,\text{mm}$, $2w = 1\,\text{mm}$, $2l = 16\,\text{mm}$, $X_{ln} = 6\,\text{mm}$ and $Z_{tr} = 0\,\text{mm}$.

The S-parameter of a slot coupled waveguide junction with $2a = 22.86\,\text{mm}$, $2b = 10.16\,\text{mm}$, $2l = 16\,\text{mm}$, $2w = 0.8\,\text{mm}$, $2t = 1.27\,\text{mm}$, $X_{ln} = 8\,\text{mm}$ and $Z_{tr} = 2\,\text{mm}$ has been compared with measured data and is shown in Figures 14 and 15.

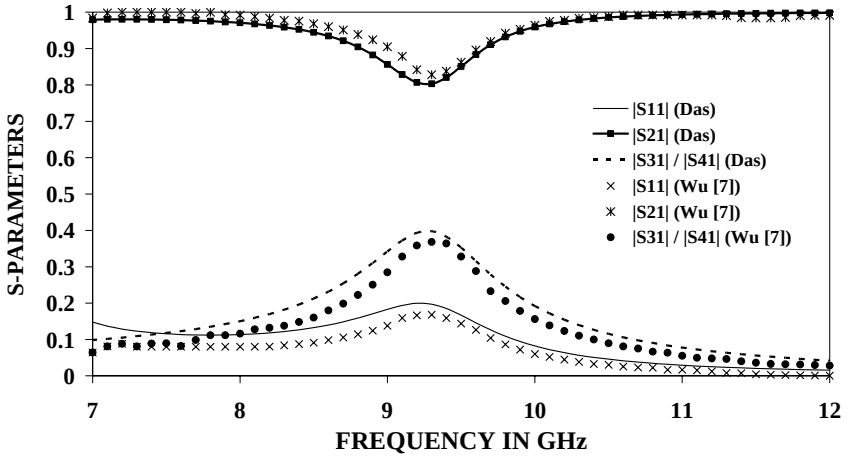


**Figure 9.** Plot of magnitude of S-parameters of a slot coupled crossed waveguide junction as a function of frequency

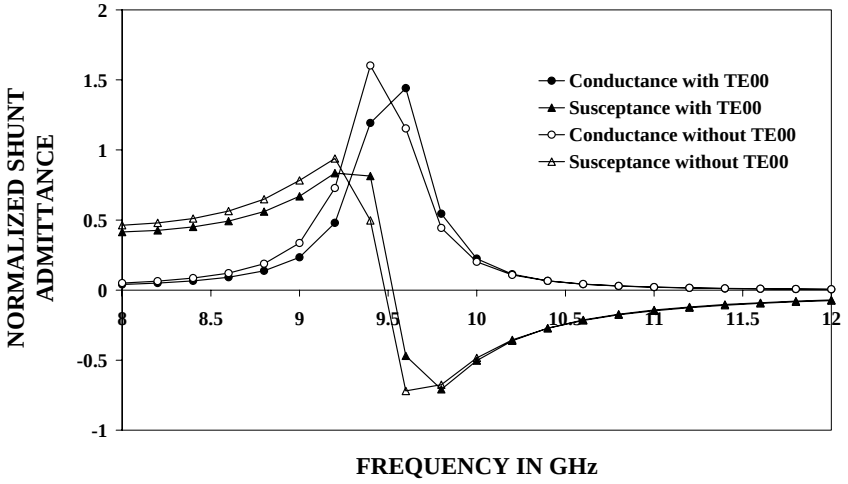


**Figure 10.** Comparison of equivalent shunt parameter with and without considering $TE_{00}$ mode.

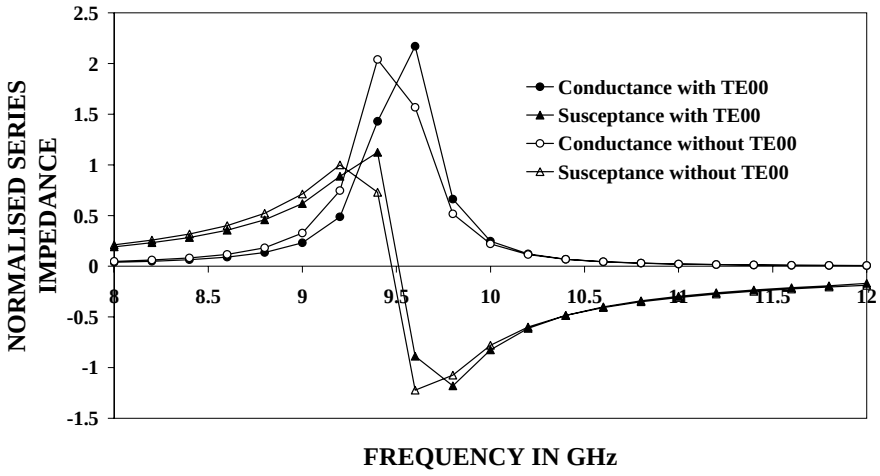


**Figure 11.** Comparison of equivalent series parameter with and without considering $TE_{00}$ mode.

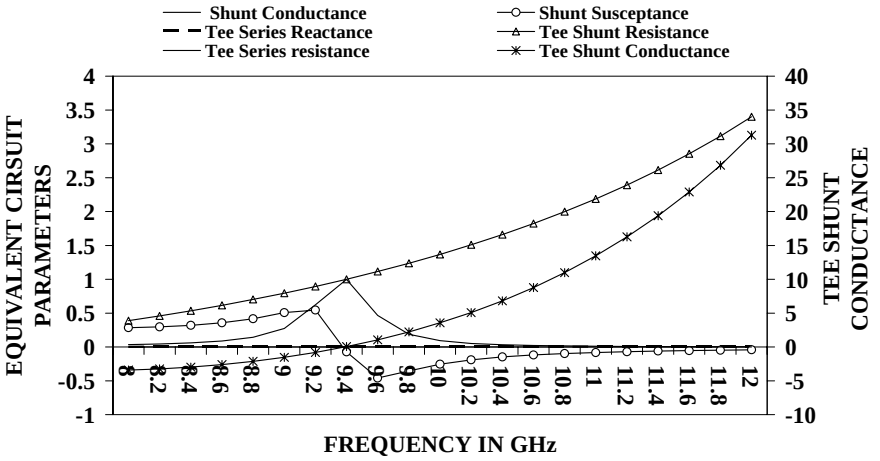


**Figure 12.** Comparison of shunt and tee network.

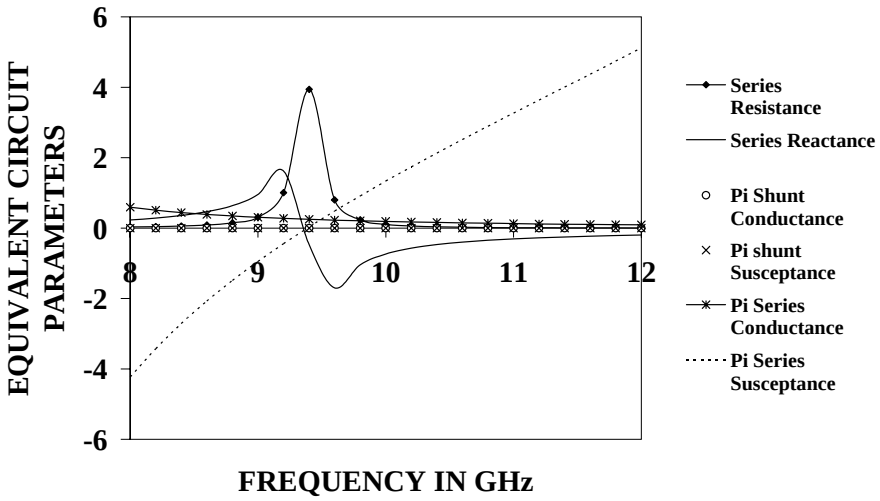


**Figure 13.** Comparison of series and pi network.

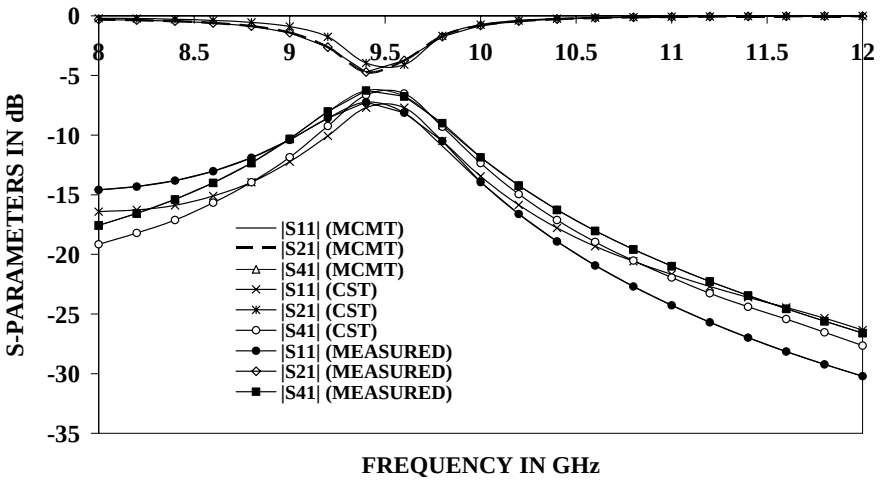


**Figure 14.** Comparison of MCMT, CST and measured data of $S_{11}, S_{21}$ and $S_{41}$.

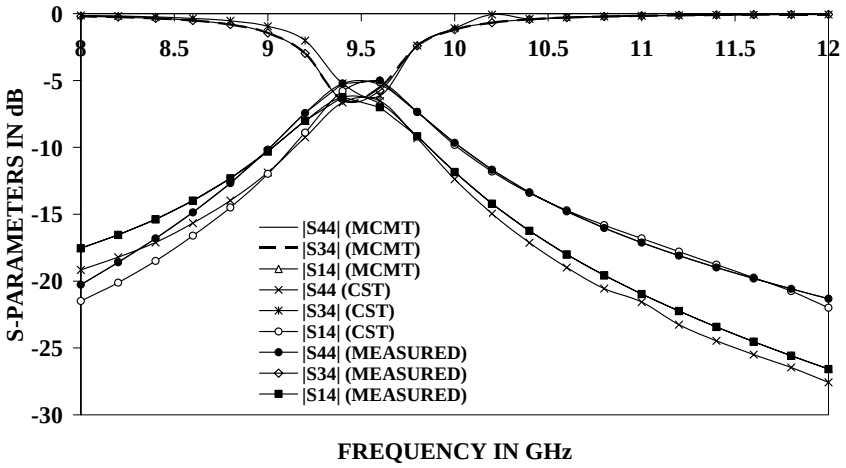


**Figure 15.** Comparison of MCMT, CST and measured data of $S_{44}, S_{34}$ and $S_{14}$.

## 4. CONCLUSION

A rigorous analysis of a longitudinal/transverse slot coupled crossed waveguide junction has been presented in this paper. The results obtained using Multiple Cavity Modeling Technique is in good agreement with the literature (Figures 5, 6 and 9)/measured and CST simulated data (Figures 14 and 15). Figures 7 and 8 reveals that the normalized resonant length decreases with increase in frequency, guide height and decrease in slot offset and slot width except for $2b = 10.16\,\text{mm}$ and slot offset less than $4.45\,\text{mm}$ when the normalized resonant length decrease with increase in slot width. From Figures 10 and 11 it is clear that $\text{TE}_{00}$ mode has an effect on the equivalent circuit of the slot coupled crossed waveguide junction and hence can not be neglected. Figure 12 reveals that the tee representation is better than the shunt representation because at resonance frequency, obtained from shunt representation, there is some non-vanishable series reactance in tee network representation. However Figure 13 shows that the series representation of the branch waveguide is acceptable because the shunt element in pi representation is zero over the entire frequency band and the series admittance is equal to the inverse of the series impedance in series representation. This is due to the fact that the coupling slot being thin, the equivalent physical length of the lossy transmission line in the branch waveguide is also very small and hence the total distributed circuit parameters can be represented by

a simple series element. However, since the slot has a considerably large electrical length (almost half of the guided wavelength) in main waveguide the equivalent physical length of the lossy transmission line in main waveguide is also large and hence it is not possible to represent the total distributed circuit parameters by a simple shunt element.

## ACKNOWLEDGMENT

This work is supported by Council of Scientific & Industrial Research, India and the authors wish to express their gratitude for this support. The Support provided by Space Technology Cell, Indian Institute of Technology, Kharagpur is also gratefully acknowledged.

## REFERENCES

1. Watson, W. H., *The Physical Principles of Waveguide Transmission and Antenna Systems*, Claredon Press, London, 1949.
2. Vu Khac, T. and C. T. Carson, "Coupling by slots in rectangular waveguides," *Electronic Letters*, Vol. 8, No. 18, 456–458, September 1972.
3. Harrington, R. F. and J. R. Mautz, "A generalized network formulation for aperture problems," *IEEE Trans. on Antennas and Propagation*, Vol. AP-24, 870–873, November 1976.
4. Rengarajan, S. R., "Characteristics of a longitudinal/transverse coupling slot in crossed rectangular waveguides," *IEEE Trans. Microwave Theory and Techniques*, Vol. 37, No. 8, 1171–1177, August 1989.
5. Park, P. K., M. E. Slaterbeck, and S. E. Bradshaw, "Shunt/series coupling slot in rectangular waveguides," *IEEE Int. Antennas and Propagation Symposium Digest*, 62–65, 1984.
6. Senior, D. C., "Higher order mode coupling effects in a shunt-series coupling junction of a planar slot array antenna," Ph.D. Dissertation, University of California, Los Angeles, CA, 1986.
7. Wu, R., D. Siru, and G. Benquing, "Analysis of a broad wall waveguide slot coupler by FDTD method," *3rd International Symposium on Electromagnetic Compatibility*, 254–258, May 21–24, 2002.
8. Das, S. and A. Chakrabarty, "A novel modeling technique to solve a class of rectangular waveguide based circuits and radiators," *Progress In Electromagnetics Research*, PIER 61, 231–252, 2006.
9. Vu Khac, T. and C. T. Carson, "$m = 0$, $n = 0$ mode

and rectangular waveguide slot discontinuity," *Electronic Letters*, Vol. 9, 431–432, September 1973.

10. Gupta, S., A. Chakrabarty, and B. N. Das, "Longitudinal slot radiators: Effect of slot offset," *International Conference on Millimeter Wave and Microwave (ICOM-90)*, DEAL, Dehradun, Dec. 19–21, 1990.
11. Satyanarayana, D. and A. Chakrabarty, "Analysis of a wide inclined slot coupled narrow wall coupler between dissimilar rectangular waveguides," *IEEE Trans. Microwave Theory and Techniques*, Vol. 42, 914–917, May 1994.
12. Satyanarayana, D. and A. Chakrabarty, "Reply to comments on analysis of a wide inclined slot coupled narrow wall coupler between dissimilar rectangular waveguides," *IEEE Trans. Microwave Theory and Techniques*, Vol. 43, 241–242, January 1995.
13. Josefsson, L. G., "Analysis of longitudinal slots in rectangular waveguides," *IEEE Trans. on Antennas and Propagation*, Vol. AP-35, 1351–1357, December 1987.
14. Gupta, S. and B. N. Das, "Analysis of longitudinal striations on the broad face of rectangular waveguides," *International Conference on Millimeter Wave and Microwave (ICOM-90)*, DEAL, Dehradun, Dec. 19–21, 1990.
15. Eshrah, I. A., A. B. Yakovlev, A. A. Kishk, A. W. Glisson, and G. W. Hanson, "The $TE_{00}$ waveguide mode — the "complete" story," *IEEE Antennas and Propagation Magazine*, Vol. 46, No. 5, October 2004.
16. Gupta, S., "Electromagnetic field estimation in aperture and slot antennas with their equivalent network representation," Ph.D. Dissertation, Department of Electronics and electrical Communication Engineering, Indian Institute of Technology, Kharagpur, India, 1996.
17. Stern, G. J. and R. S. Elliot, "Resonant length of longitudinal slots and validity of circuit representation: theory and experiment," *IEEE Trans. on Antennas and Propagation*, Vol. AP-33, 1264–1271, November 1985.
18. Rengarajan, S. R., "Compound radiating slots in the broad wall of a rectangular waveguide," *IEEE Trans. on Antennas and Propagation*, Vol. 37, No. 9, 1116–1123, September 1989.
19. Rengarajan, S. R., "Compound coupling slots for arbitrary excitation of waveguide-fed planar slot arrays," *IEEE Trans. on Antennas and Propagation*, Vol. 38, No. 2, 276–280, February 1990.

20. Casula, G. A., G. Mazzarella, and G. Montisci, "A new circuital model for the longitudinal-transverse waveguide slot coupler," *Microwave and Optical Technology Letters*, Vol. 44, No. 2, 313–318, February 20, 2005.